

# Thermodynamics of quantum jump trajectories in systems driven by classical fluctuations

Adrián A. Budini

*Consejo Nacional de Investigaciones Científicas y Técnicas,  
Centro Atómico Bariloche, Av. E. Bustillo Km 9.5, (8400) Bariloche, Argentina*

(Dated: August 3, 2018)

The large-deviation method can be used to study the measurement trajectories of open quantum systems. For optical arrangements this formalism allows to describe the long time properties of the (non-equilibrium) photon counting statistics in the context of a (equilibrium) thermodynamic approach defined in terms of dynamical phases and transitions between them in the trajectory space [J.P. Garrahan and I. Lesanovsky, *Phys. Rev. Lett.* **104**, 160601 (2010)]. In this paper, we study the thermodynamic approach for fluorescent systems coupled to complex reservoirs that induce stochastic fluctuations in their dynamical parameters. In a fast modulation limit the thermodynamics corresponds to that of a Markovian two-level system. In a slow modulation limit, the thermodynamic properties are equivalent to those of a finite system that in an infinite-size limit is characterized by a first-order transition. The dynamical phases correspond to different intensity regimes, while the size of the system is measured by the transition rate of the bath fluctuations. As a function of a dimensionless intensive variable, the first and second derivative of the thermodynamic potential develop an abrupt change and a narrow peak respectively. Their scaling properties are consistent with a double-Gaussian probability distribution of the associated extensive variable.

PACS numbers: 05.70.Ln, 03.65.Yz, 05.30.-d, 42.50.Lc

## I. INTRODUCTION

The interaction of small quantum systems with an infinite set of uncontrollable degrees of freedom leads to non-equilibrium time irreversible evolutions. This is the main topic of the theory of open quantum systems [1]. In this context, a diverse kind of physical systems can be described through a quantum master equation, which defines the dynamics of their density matrix operators.

Quantum optical arrangements fall in the previous category [2–6]. The irreversible dynamics is induced by the background electromagnetic field, which leads to the natural radiative decay of the system. The opposite mechanism, where the system becomes excited to higher energy levels, can be induced by the interaction with an external laser field. The competition between both effects produces a continuous emission of photons.

The detection of the radiated photons occurs at random times. Successive measurement realizations provide an ensemble of trajectories, which define a stochastic (point) process [7]. Its statistics can be described through different approaches, such as generating operator techniques [8], or the quantum jump approach [1–4]. These formalisms can also be utilized in the description of fluorescent systems coupled to classically fluctuating reservoirs [9–11]. The interaction with the bath is modeled through a set of random processes that modify the characteristic parameters of the system [12–16]. In these cases, the main task is to relate the environment fluctuations with the photon-counting statistics [9–20].

In contrast to the previous approaches, statistical mechanics provides the theoretical tools for describing systems in thermal equilibrium [21]. It allows to get the dependence of extensive thermodynamic observables as

a function of the conjugate (intensive) variables. Phase transition points are defined by nonanalyticities of a thermodynamic potential in the parameter space.

While both non-equilibrium (small) quantum systems and thermodynamic ones are described with intrinsically different approaches, in a recent contribution Garrahan and Lesanovsky related both kind of descriptions [22]. The bridge between both areas is provided by the large-deviation (LD) theory [23]. This formalism is concerned with the exponential decay of probabilities corresponding to large fluctuations in a stochastic system. It allows to describe its ensemble of trajectories in the same way as equilibrium statistical mechanics describes ensemble of configurations in phase space [23–27]. The role of the thermodynamic variables is played by dynamical order parameters or their associated conjugate fields. The existence of “space-time” phase transitions in glassy systems [28] was established through this approach.

We notice that the dynamic and physical properties, such as subPoissonian photon statistic, photon-antibunching, spectrum peaks (Mollow triplet), squeezed noise, bistability, etc., that can be found in quantum optical systems are very well known [5, 6]. The breakthrough introduced in Ref. [22] is not directly related with those phenomena. The main idea was to apply the LD formalism to the measurement trajectories of simple open quantum systems, such as (two) three-level fluorescent systems and a micromaser. The extra physical aspect that can be analyzed with the LD approach is the asymptotic (long time) statistical properties of the measurement trajectories, such as for example the statistic of the number of detected photons in the case of fluorescent systems or the number of atoms leaving the cavity in a given state for the micromaser. The LD approach,

by going beyond the central limit theorem [23], allows to describe the asymptotic regime with a set of functions that in a statistical mechanics interpretation play the role of entropy and free energy. By modifying the system parameters and a conjugate dimensionless (dynamical) order parameter, properties such as scale invariance points, crossover between distinct dynamical phases, and an actual first-order phase transition were found in the thermodynamic approach [22]. As these properties are related with physical observables defined from the ensemble of measurement trajectories they should be detectable in experiments.

The main goal of this paper is to extend the analysis of Ref. [22] to the case of fluorescent systems coupled to complex self-fluctuating reservoirs. The system-bath dynamics is described through a density matrix formalism [19, 20]. Our interest is to characterize the thermodynamic formalism associated to the photon counting probabilities as a function of the statistical properties of the environment fluctuations. We show that in a fast modulation limit, i.e., when the characteristic time of the bath fluctuations is the minor time scale of the problem, the thermodynamic frame reduces to that of a Markovian fluorescent two-level system. A scale invariance point is recovered for a special set of system parameter values. On the other hand, in a slow modulation limit the thermodynamical properties of the measurement trajectories are equivalent to those of finite systems that in an infinite-size limit develop a first-order phase transition [29–32]. Here, the phases are related with different intensity regimes of the scattered radiation, while the (thermodynamic) size of the system is associated to the characteristic rate of the bath fluctuations. The finite-size effects are similar to those found in the Ising or q-state Potts models [31, 32]. These properties are shown through the thermodynamical response functions, i.e., the first and second derivatives of the thermodynamic potential with respect to an intensive parameter.

The paper is outlined as follows. In Sec. II, based on the theoretical results established in Ref. [22], we define the thermodynamic approach for an arbitrary counting process. In Sec. III we define the density matrix evolution and photon counting statistics of the system of interest, i.e., a fluorescent (two-level) system driven by classical fluctuations. In Sec. IV we analyze the thermodynamic approach in the limit of fast environment fluctuations, while the case of slow fluctuations is developed in Sec. V. The conclusions are presented in Sec. VI.

## II. THERMODYNAMICS OF COUNTING PROCESSES

Here, we define the thermodynamic formalism [22] for an arbitrary counting process [7]. In the next section, it is build up from the photon statistics of a fluorescent system driven by classical fluctuations.

A counting process is defined by a set of trajectories,

each one consisting in a series of consecutive events occurring at random times [7]. It can be statistically characterized by a set of probabilities  $\{P_n(t)\}_{n=0}^{\infty}$ , satisfying  $0 \leq P_n(t) \leq 1$ , and the normalization

$$\sum_{n=0}^{\infty} P_n(t) = 1. \quad (1)$$

Each  $P_n(t)$  is the probability of occurrence of  $n$ -events up to time  $t$ . From these objects, we introduce an associated stochastic process defined by the probabilities

$$q_n(t) \equiv \frac{1}{Z_t(s)} P_n(t) e^{-sn}, \quad (2)$$

where  $s$  is a real parameter. Consistently with the condition  $\sum_{n=0}^{\infty} q_n(t) = 1$ , the function  $Z_t(s)$  is defined by

$$Z_t(s) \equiv \sum_{n=0}^{\infty} P_n(t) e^{-sn}. \quad (3)$$

Hence,  $Z_t(s)$  is the generating function [7] of the original counting process,

$$Z_t(s) = \langle\langle \exp[-sn_{st}(t)] \rangle\rangle_{\{P\}}. \quad (4)$$

Here,  $n_{st}(t)$  is the (stochastic) number of events up to time  $t$  in a given realization while  $\langle\langle \dots \rangle\rangle_{\{P\}}$  denotes an average over the realizations associated to the set  $\{P_n(t)\}_{n=0}^{\infty}$ .

From the transformation (2), one can deduce that unlikely events of the counting process  $\{P_n(t)\}_{n=0}^{\infty}$  becomes typical events in the  $s$ -ensemble [23], i.e., in the set of realizations defined by the probabilities  $\{q_n(t)\}_{n=0}^{\infty}$ . At each time  $t$ , the rare events has associated a thermodynamic-like structure. The consistency of this affirmation becomes evident after introducing the corresponding statistical objects. A thermodynamic entropy function  $S_t$  can be defined as the Shannon entropy of the  $s$ -ensemble,

$$S_t \equiv - \sum_{n=0}^{\infty} q_n(t) \log[q_n(t)]. \quad (5)$$

By reading the function  $Z_t(s)$  as a partition function [21], we define a “free energy function” or “grand (thermodynamic) potential” as

$$\Theta_t \equiv - \log[Z_t(s)]. \quad (6)$$

A “internal energy” is defined as

$$\langle\langle E \rangle\rangle_t \equiv - \sum_{n=0}^{\infty} q_n(t) \log[P_n(t)], \quad (7)$$

while the “average particle number” reads

$$\langle\langle N \rangle\rangle_t \equiv \sum_{n=0}^{\infty} q_n(t) n. \quad (8)$$

Then, it is straightforward to relate the previous objects through the thermodynamic relation

$$\Theta_t = \langle\langle E \rangle\rangle_t - S_t + s\langle\langle N \rangle\rangle_t. \quad (9)$$

In fact, in units of energy where  $kT = 1$ ,  $k$  denoting the Boltzmann constant and  $T$  temperature, and defining a (dimensionless) “chemical potential”  $\mu \equiv -s$ , the previous relation arises in the description of thermodynamical (equilibrium) processes carried out in open systems that can exchange both heat and matter with their surroundings [21]. Therefore, both the energy and particle number can fluctuate. Consistently with a statistical derivation based on maximizing entropy,  $\langle\langle E \rangle\rangle_t$  and  $\langle\langle N \rangle\rangle_t$  can be read as the constraints on the average energy and particle number respectively. Here, the average, denoted as  $\langle\langle \dots \rangle\rangle_t$ , is defined by the set of probabilities  $\{q_n(t)\}_{n=0}^\infty$ .

The thermodynamic interpretation allows us to write the average number (extensive variable) as the derivative of the (pseudo) grand potential  $\Theta_t$  with respect to the (pseudo) chemical potential  $s$  [21] (intensive variable),

$$\langle\langle N \rangle\rangle_t = \frac{\partial}{\partial s} \Theta_t, \quad (10)$$

while the average of the centered quadratic fluctuations follows from the second derivative,

$$\langle\langle \Delta N^2 \rangle\rangle_t \equiv \langle\langle N^2 \rangle\rangle_t - \langle\langle N \rangle\rangle_t^2 = -\frac{\partial^2}{\partial s^2} \Theta_t. \quad (11)$$

These (two) thermodynamic relations can alternatively be derived by writing  $\langle\langle N \rangle\rangle_t$  and  $\langle\langle \Delta N^2 \rangle\rangle_t$  as the average and variance of the number of events up to time  $t$  associated to the set of probabilities  $\{q_n(t)\}_{n=0}^\infty$ .

The thermodynamic frame [Eq. (9)] is parametrized by the time  $t$ . In a long time regime, for ergodic processes, it is expected that all averaged quantities (strictly, all cumulants) become proportional to the evaluation time  $t$ . Hence, the normalized asymptotic average values

$$\langle\langle \dots \rangle\rangle \equiv \lim_{t \rightarrow \infty} \frac{1}{t} \langle\langle \dots \rangle\rangle_t, \quad (12)$$

become time independent. In this regime, the partition function acquires a LD form [22]

$$\lim_{t \rightarrow \infty} Z_t(s) \approx \exp[-t\Theta(s)]. \quad (13)$$

Then, the previous relations [Eqs. (10) and (11)] maintain their validity after replacing  $\Theta_t \rightarrow \Theta(s)$  and  $\langle\langle \dots \rangle\rangle_t \rightarrow \langle\langle \dots \rangle\rangle$ . Notice that  $\Theta(s)$  and all normalized average values  $\langle\langle \dots \rangle\rangle$  have units of [1/time].

The pseudo-thermodynamic structure defined previously is associated to the probabilities (2). The LD formalism allows to relate it with an observable property of the original counting process, i.e., with the long time behavior of the probabilities  $\{P_n(t)\}_{n=0}^\infty$ . Consistently with Eq. (13), their asymptotic structure is written as  $\lim_{t \rightarrow \infty} P_n(t) \approx \exp[-t\varphi(\frac{n}{t})]$ . Taking into account that the LD function  $\varphi(N)$  ( $N = n/t$ ) also defines the asymptotic behavior of the internal energy (7)

and entropy (5), it can be related to the grand potential through a Legendre-Fenchel transformation [22, 23],  $\varphi(N) = \max_s[\Theta(s) - sN]$ , which in turn guarantees that  $\Theta(s)$  has convexity properties consistent with the thermodynamical interpretation.

From the previous relations, it becomes evident that the thermodynamical potential  $\Theta(s)$  provide an alternative and complete characterization of the asymptotic properties of the set  $\{P_n(t)\}_{n=0}^\infty$ . In consequence, possible phase transitions happening in the thermodynamic frame must to be related to strong modifications in the statistical properties of the original counting process. These relations and its associated theoretical frame provide an alternative and novel approach for analyzing measurement trajectories of single open quantum systems subjected to a continuous measurement process [22].

### III. FLUORESCENT SYSTEMS DRIVEN BY CLASSICAL FLUCTUATIONS

In many nanoscopic optical systems, such as those analyzed in the context of single-molecule spectroscopy [9–11], the randomness of the photon emission process arises from both the interaction with the background electromagnetic field and intrinsic environment fluctuations. This last effect can be modeled by a set of noises that modify (modulate) the parameters of the system evolution [12–16]. As demonstrated in Refs. [19, 20], the noises modeling can be reformulated through a density matrix formalism. Here, we present a short derivation of both the underlying density matrix evolution and the photon counting statistics.

The environment is defined by a set of (configurational) macrostates, each one leading to a different system dynamics. The transitions between the bath states is described by a classical rate equation [7]

$$\frac{dP_R(t)}{dt} = \sum_{R'} \phi_{RR'} P_{R'}(t) - \sum_{R'} \phi_{R'R} P_R(t), \quad (14)$$

where  $P_R(t)$  is the probability of finding the environment in a given state  $R = 1, \dots, R_{\max}$ , at time  $t$ . The set  $\{\phi_{RR'}\}$  define the hopping rates. The system density matrix  $\rho(t)$  is described by a set of auxiliary states  $\{\rho_R(t)\}$ , each one representing the system dynamic for each bath state. Then, by writing

$$\rho(t) = \sum_R \rho_R(t), \quad (15)$$

and demanding the condition

$$\text{Tr}[\rho_R(t)] = P_R(t), \quad (16)$$

where  $\text{Tr}[\dots]$  denotes a trace operation in the system

Hilbert space, we introduce the evolution [19]

$$\begin{aligned} \frac{d\rho_R(t)}{dt} = & \frac{-i}{\hbar}[H_R, \rho_R(t)] + \gamma_R \mathcal{L}[\rho_R(t)] \\ & + \sum_{R'} \phi_{RR'} \rho_{R'}(t) - \sum_{R'} \phi_{R'R} \rho_R(t). \end{aligned} \quad (17)$$

The last line of this equation introduce a coupling between the auxiliary states and takes into account the environment fluctuations. The constant  $\gamma_R$  define the natural decay of the system associated to each  $R$ -bath state. Consistently, the Lindblad superoperator  $\mathcal{L}[\bullet]$  reads [1]

$$\mathcal{L}[\bullet] = -\frac{1}{2}\{\sigma^\dagger \sigma, \bullet\}_+ + \sigma \bullet \sigma^\dagger, \quad (18)$$

where  $\{\dots\}_+$  denotes an anticommutation operation. The operator  $\sigma$  ( $\sigma^\dagger$ ) is the lowering (raising) operator between the system eigenstates. It is modeled through a two-level optical transition with eigenstates  $\{|\pm\rangle\}$ . Then,  $\sigma = |-\rangle\langle +|$  and  $\sigma^\dagger = |+\rangle\langle -|$ .

In the first line of Eq. (17),  $H_R$  is the system Hamiltonian associated to each bath state. It reads [19, 20]

$$H_R = \frac{\hbar\omega_R}{2}\sigma_z + \frac{\hbar\Omega_R}{2}(\sigma^\dagger e^{-i\omega_L t} + \sigma e^{+i\omega_L t}), \quad (19)$$

where  $\sigma_z$  is the  $z$ -Pauli matrix in the basis  $\{|\pm\rangle\}$ , and  $\omega_R = \omega_0 + \delta\omega_R$ . Therefore,  $\omega_0$  defines the bare transition frequency of the system, while  $\delta\omega_R$  are the spectral shifts induced by the interaction with the bath. The second contribution takes into account the interaction with the external laser field.  $\Omega_R$  is the effective Rabi frequency associated to each reservoir state, while  $\omega_L$  is the frequency of the external laser excitation.

The sum structure Eq. (15), added to the local character of the evolution (17), imply the presence of strong non-Markovian effects in the system dynamics [19]. On the other hand, Eq. (17) does not take into account light assisted processes. While these phenomena appear in real experimental situations [9–11], most of the results developed in the next sections can be easily extended to include such kind of effects [19, 20].

### Photon-counting statistics

The photon detection statistics can be obtained by expressing the system density matrix (15) as

$$\rho(t) = \sum_{n=0}^{\infty} \rho^{(n)}(t). \quad (20)$$

Each state  $\rho^{(n)}(t)$  corresponds to the system state conditioned to  $n$ -photons detection events [2, 3]. The probability of counting  $n$ -photons up to time  $t$  reads

$$P_n(t) = \text{Tr}[\rho^{(n)}(t)]. \quad (21)$$

This set of probabilities can be obtained through a generating function approach [7]. Due to the quantum nature

of the system, a “generating operator” is introduced

$$\mathcal{G}(t, s) \equiv \sum_{n=0}^{\infty} e^{-sn} \rho^{(n)}(t), \quad (22)$$

where the extra real parameter  $s$  plays the same role as in Eq. (2). The partition function Eq. (3) follow as

$$Z_t(s) = \text{Tr}[\mathcal{G}(t, s)]. \quad (23)$$

From the equality  $\rho(t) = \mathcal{G}(t, s)|_{s=0}$ , the condition  $Z_t(s)|_{s=0} = 1$  is consistently satisfied.

The conditional states  $\rho^{(n)}(t)$  can be decomposed into the contributions associated to each configurational state of the reservoir, leading to the expression

$$\mathcal{G}(t, s) = \sum_{n=0}^{\infty} e^{-sn} \sum_R \rho_R^{(n)}(t) \equiv \sum_R \mathcal{G}_R(t, s). \quad (24)$$

Each matrix  $\rho_R^{(n)}(t)$  defines the state of the system under the condition that at time  $t$   $n$ -photon detection events happened, and the environment is in the configurational state  $R$ . Consistently, each contribution  $\mathcal{G}_R(t, s)$  defines the (conditional) generating operator “given” that the reservoir is in the  $R$ -state. Its evolution reads [19]

$$\begin{aligned} \frac{d\mathcal{G}_R(t, s)}{dt} = & \frac{-i}{\hbar}[H_R, \mathcal{G}_R(t, s)] + \gamma_R \mathcal{L}_s[\mathcal{G}_R(t, s)] \\ & + \sum_{R'} \phi_{RR'} \mathcal{G}_{R'}(t, s) - \sum_{R'} \phi_{R'R} \mathcal{G}_R(t, s), \end{aligned} \quad (25)$$

where the superoperator  $\mathcal{L}_s$  is given by

$$\mathcal{L}_s[\bullet] = -\frac{1}{2}\{\sigma^\dagger \sigma, \bullet\}_+ + e^{-s} \sigma \bullet \sigma^\dagger. \quad (26)$$

The evolution (25) can be solved in a Laplace domain. From Eq. (24), the partition function (23) can always be written as a quotient of two polynomial functions,  $Z_u(s) = f(u)/g(u)$ , where  $u$  is the Laplace variable. Then, by using the residues theorem, the grand potential  $\Theta(s)$  [Eq. (13)] follows from the larger root of the equation  $g(u) = 0$ . This property allows us to get all objects characterizing the  $s$ -ensemble. In the following section we study its associated statistic in a fast and slow modulation limits.

In Ref. [22] it was demonstrated that it is always possible to find a density matrix  $\tilde{\rho}(t)$  whose associated measurement statistics is given by the probabilities  $q_n(t)$ , Eq. (2). In the present context, one can affirm that the  $s$ -ensemble statistics can be recovered from a set of auxiliary states  $\{\tilde{\rho}_R(t)\}_{R=1}^{R_{\max}}$  defined as

$$\tilde{\rho}_R(t) = \frac{l_R^{1/2} \rho_R(t) l_R^{1/2}}{\sum_R \text{Tr}[l_R \rho_R(t)]}, \quad (27)$$

where the set of operators  $\{l_R\}$  is the left “eigenoperator” of the evolution (25).

#### IV. FAST MODULATION LIMIT

The thermodynamic frame associated to Eq. (23) in general cannot be characterized in an analytical way. Nevertheless, in the limit of fast and slow environment fluctuations the problem becomes analytically treatable.

For the original ensemble of trajectories [Eq. (21)], the fast modulation limit refers to the case in which the environment transitions are much faster than the photon emission process. From Eq. (17), this condition can explicitly be written as

$$\{\phi_{RR'}\} \gg \{I_R\}. \quad (28)$$

The constant  $I_R$  is the intensity associated to the  $R$ -bath state [diagonal contribution in (17)], i.e., the intensity of a Markovian two-level system with natural decay  $\gamma_R$ , Rabi frequency  $\Omega_R$ , and detuning  $\delta_R$  [19, 20],

$$I_R = \frac{\gamma_R \Omega^2}{\gamma_R^2 + 2\Omega^2 + 4\delta_R^2}, \quad (29)$$

where  $\delta_R \equiv \omega_L - \omega_R$ . Both,  $\omega_L$  and  $\omega_R$  are defined from Eq. (19). The inequality (28) implies that the average time between two consecutive photon emissions is much larger than the characteristic time of the bath fluctuations. Under this condition, the fluorescent system can be approximated by a Markovian system whose evolution is defined by the average parameters [16, 19]

$$\gamma = \sum_R P_R^\infty \gamma_R, \quad \omega = \sum_R P_R^\infty \omega_R, \quad \Omega = \sum_R P_R^\infty \Omega_R. \quad (30)$$

The weights  $\{P_R^\infty\}$  are the stationary solution of (14),

$$P_R^\infty \equiv \lim_{t \rightarrow \infty} P_R(t). \quad (31)$$

Therefore, the generating operator [Eq. (24)] can be approximated as

$$\mathcal{G}(t, s) \simeq \mathcal{G}_M(t, s), \quad (32)$$

where  $\mathcal{G}_M(t, s)$  is defined by the Markovian evolution

$$\frac{d\mathcal{G}_M(t, s)}{dt} = -\frac{i}{\hbar} [H, \mathcal{G}_M(t, s)] + \gamma \mathcal{L}_s[\mathcal{G}_M(t, s)]. \quad (33)$$

Here,  $\mathcal{L}_s[\bullet]$  follows from Eq. (26) while  $H$  can be read from Eq. (19) after replacing  $\omega_R \rightarrow \omega$  and  $\Omega_R \rightarrow \Omega$ . The sub-index  $M$  indicates the underlying Markovian approximation.

From Eqs. (13) and (23), it is possible to associate a thermodynamic potential  $\Theta_M(s)$  to the operator  $\mathcal{G}_M(t, s)$ . Its thermodynamics cumulants are

$$\langle\langle N \rangle\rangle_M = \frac{\partial \Theta_M(s)}{\partial s}, \quad \langle\langle \Delta N^2 \rangle\rangle_M = -\frac{\partial^2 \Theta_M(s)}{\partial s^2}. \quad (34)$$

The analytical expression for  $\Theta_M(s)$  that can be obtained from Eq. (33) correspond to the larger root of a

fourth degree polynomial. When the external laser excitation is in resonance with the (Markovian) system, i.e.,  $\omega_L = \omega$ , the polynomial is of third order. Thus, the expression for  $\Theta_M(s)$  becomes much more simple. Under the previous condition, from Eqs. (13) and (23), we get

$$\Theta_M(s) = \frac{\gamma}{2} - \frac{1}{6} f(s) + \frac{4\Omega^2 - \gamma^2}{2f(s)}. \quad (35)$$

The auxiliary function  $f(s)$ , after introducing the ‘‘fugacity’’  $z \equiv \exp(-s)$  [21], reads

$$f(s) = \left( 54z\gamma\Omega^2 + \sqrt{(54z\gamma\Omega^2)^2 + 27(4\Omega^2 - \gamma^2)^3} \right)^{1/3}. \quad (36)$$

Notice that when  $\gamma = 2\Omega$  it follows  $\Theta_M = \Omega(1 - e^{-s/3})$ , which recovers the result presented in Ref. [22]. It is characterized by the scale invariant property  $\langle\langle \Delta N^2 \rangle\rangle_M / \langle\langle N \rangle\rangle_M = 1/3$ , i.e., the normalized fluctuations do not depend on  $s$ .

In Fig. 1, we characterize the thermodynamic frame associated to Eqs. (17) and (25) in the fast modulation limit. We assume a two-dimensional configurational space, i.e., the bath is characterized by only two states,  $R = A, B$ . We take  $\omega_R = \omega_0$  and  $\Omega_R = \Omega$ , i.e., the spectral shifts are null and the system-laser interaction is independent of the bath states. Hence, the reservoir only affects the natural decay of the system,  $\{\gamma_R\}$ . Furthermore, the laser excitation is assumed to be in resonance with the system,  $\omega_L = \omega_0$ . Under these conditions, we can approximate the grand potential as  $\Theta(s) \approx \Theta_M(s)$  [Eqs. (35)].

In Fig. 1(a) we plot the average number  $\langle\langle N \rangle\rangle$ . In the inset, we show the corresponding grand thermodynamic potential, which is obtained as the larger root of an eighth order polynomial function. For the chosen parameter values, the fast modulation limit is achieved for all values of  $s$ . In fact, in both cases the curves are indistinguishable from the analytical expressions Eqs. (35) and (34). The average rate [Eq. (30)] is indicated in the plots. Notice that for the upper (blue filled squares) curve  $\gamma/\Omega > 2$ , while for the lower (red filled circles) curve  $\gamma/\Omega < 2$ . Each value corresponds respectively to an overdamped [ $2 < \gamma/\Omega < \infty$ ] and underdamped [ $0 < \gamma/\Omega < 2$ ] regimes of the Markovian dynamics, Eq. (33).

In Fig. 1(b) we plot the normalized fluctuations  $\langle\langle \Delta N^2 \rangle\rangle / \langle\langle N \rangle\rangle$ . This function is almost indistinguishable from the fitting that follows from Eqs. (35) and (34). In the limit  $s \rightarrow +\infty$ , asymptotically all curves converge to 1. This property is fulfilled by a Poisson process [7]. In the limit  $s \rightarrow -\infty$ , all curves converge to 1/3, i.e., the value of the scale invariant regime [22]. In the curves associated to the red filled circles and blue filled squares the parameters are the same than in Fig. 1(a). On the other hand, the extra curves associated to the red empty circles and blue empty squares correspond to a different set of parameter values that also are in the underdamped and overdamped regimes respectively. From these curves we deduce that, in both regimes, when  $\gamma/\Omega \rightarrow 2$  the transition between 1/3 and 1 occurs for higher values of the

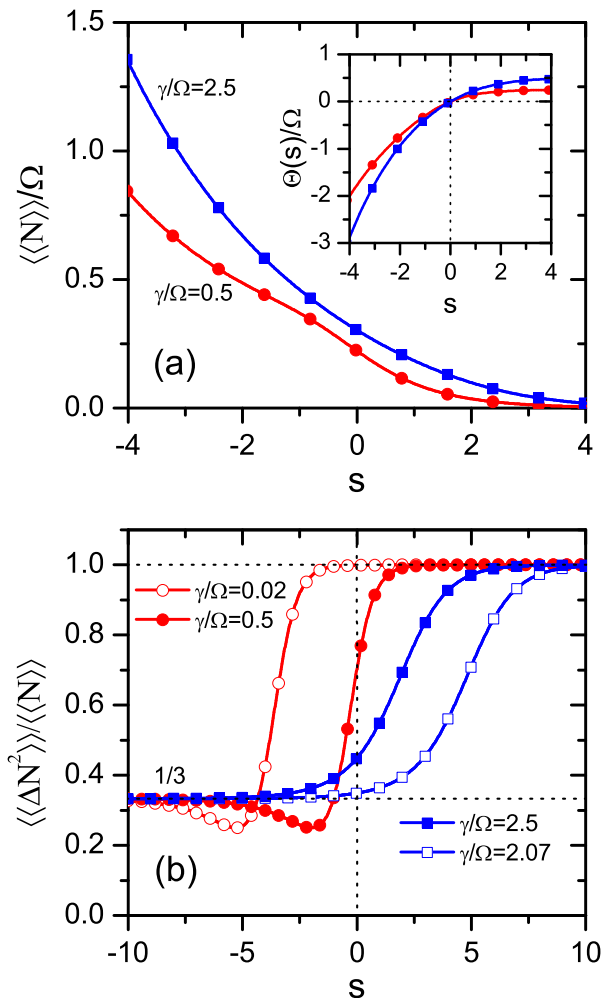


FIG. 1: (color online) (a) Average number value  $\langle\langle N \rangle\rangle$  as a function of the chemical potential  $s$  in the fast modulation limit. The inset show the respective grand potential  $\Theta(s)$ . (b) Plot of the normalized fluctuations  $\langle\langle \Delta N^2 \rangle\rangle / \langle\langle N \rangle\rangle$ . All curves are almost indistinguishable with the fitting defined by Eqs. (34) and (35). The parameters of the Hamiltonian dynamics are  $\omega_R = \omega_0$  and  $\Omega_R = \Omega$ , while for the irreversible one read  $\gamma_A/\Omega = 2$ ,  $\gamma_B/\Omega = 3$  (blue filled squares), and  $\gamma_A/\Omega = 0.3$ ,  $\gamma_B/\Omega = 0.7$  (red filled circles). In (b), the parameters of the extra curves are  $\gamma_A/\Omega = 2.5$ ,  $\gamma_B/\Omega = 1.64$  (blue empty squares), and  $\gamma_A/\Omega = 0.01$ ,  $\gamma_B/\Omega = 0.03$  (red empty circles). In all cases we take  $\phi_{AB}/\Omega = \phi_{BA}/\Omega = 10$ . The average decay rate, Eq. (30), is written in each plot.

chemical potential,  $s \rightarrow +\infty$ . Furthermore, we checked that when  $\gamma/\Omega = 2$  a scale invariance property [22] is recovered,  $\langle\langle \Delta N^2 \rangle\rangle / \langle\langle N \rangle\rangle = 1/3$ . The validity of this behavior occurs for increasing values of the rates  $\phi_{RR'}$ .

## V. SLOW MODULATION LIMIT

When  $\{\phi_{RR'}\} \ll \{I_R\}$ , the system is able to emits a huge quantity of photons before a bath transition occurs

[16, 19, 20]. Therefore, the photon emission process develops a blinking property, i.e., the intensity randomly changes between the set of values  $\{I_R\}$ . Each change in the intensity regime can be associated to a bath configurational transition. This limit is much more interesting than the previous one. Signatures of a thermodynamical phase transition can be found in this regime. First, we describe the emission process through a stochastic approximation. In a second step, we characterize the thermodynamic associated to the  $s$ -ensemble.

### A. Stochastic approach

In the slow modulation limit, the realizations of the photon counting process [i.e., the realizations associated to the probabilities (21)] can be approximated by the stochastic process

$$n_{st}(t) = \sum_R \int_0^t d\tau \delta_{RR_{st}(\tau)} \frac{dn_R^{st}(\tau)}{d\tau}. \quad (37)$$

As in Eq. (4),  $n_{st}(t)$  is the (stochastic) number of photon detection events up to time  $t$ . On the other hand,  $R_{st}(\tau) \in (1, \dots, R_{\max})$  is a random process that indicates which is the state of the reservoir at time  $\tau$ . Then, the contribution defined by the discrete delta function  $\delta_{RR_{st}(\tau)}$  does not vanish only when  $R_{st}(\tau) = R$ , where it is equal to 1. Finally,  $n_R^{st}(\tau)$  is the (stochastic) number of photon recording events up to time  $\tau$  corresponding to a Markovian fluorescent system defined by the decay rate  $\gamma_R$ , transition frequency  $\omega_R$ , and Rabi frequency  $\Omega_R$ , i.e., the parameters associated to each reservoir state.

Consistently with the slow modulation limit, we can assume that  $R_{st}(\tau)$  and the set  $\{n_R^{st}(\tau)\}$  are statistically independent between all them. Hence, the average number follows from Eq. (37) as

$$\langle\langle n_{st}(t) \rangle\rangle_{\{P\}} = \sum_R \int_0^t d\tau \langle \delta_{RR_{st}(\tau)} \rangle \frac{d\overline{n_R^{st}(\tau)}}{d\tau}. \quad (38)$$

With  $\langle \dots \rangle$  and the overbar  $\overline{(\dots)}$  symbols we denote an average over the realizations of  $R_{st}(t)$  and  $n_R^{st}(t)$  respectively. Trivially, one can write  $\langle \delta_{RR_{st}(\tau)} \rangle = P_R(\tau)$ , where  $\{P_R(t)\}$  are the solution of Eq. (14). After assuming that  $\overline{n_R^{st}(0)} = 0$  and  $P_R(0) = P_R^\infty$  [Eq. (31)], we get

$$\langle\langle n_{st}(t) \rangle\rangle_{\{P\}} = \sum_R P_R^\infty \overline{n_R^{st}(t)}. \quad (39)$$

Therefore, the average number  $\langle\langle n_{st}(t) \rangle\rangle_{\{P\}}$  can be written as a linear combination of the averages  $\{\overline{n_R^{st}(t)}\}$ , each one being weighted by the stationary configurational populations  $\{P_R^\infty\}$ . Taking into account that  $\overline{n_R^{st}(t)} = I_R t$ , the normalized asymptotic average value  $\langle\langle \Delta n_{st} \rangle\rangle_{\{P\}} \equiv \lim_{t \rightarrow \infty} (1/t) \langle\langle \Delta n_{st}(t) \rangle\rangle_{\{P\}}$ , trivially reads

$$\langle\langle n_{st} \rangle\rangle_{\{P\}} = \sum_R P_R^\infty I_R. \quad (40)$$

The second cumulant, defined by

$$\langle\langle \Delta n_{st}^2(t) \rangle\rangle_{\{P\}} \equiv \langle\langle n_{st}^2(t) \rangle\rangle_{\{P\}} - \langle\langle n_{st}(t) \rangle\rangle_{\{P\}}^2, \quad (41)$$

can be obtained in a similar way. First, from Eq. (37) we write the second moment as

$$\begin{aligned} \langle\langle n_{st}^2(t) \rangle\rangle_{\{P\}} &= 2 \sum_{RR'} \int_0^t d\tau \int_0^\tau d\tau' \langle \delta_{RR_{st}(\tau)} \delta_{R'R_{st}(\tau')} \rangle \\ &\quad \frac{d}{d\tau} \frac{d}{d\tau'} \overline{[n_R^{st}(\tau) n_{R'}^{st}(\tau')]}. \end{aligned} \quad (42)$$

The average appearing in the first line can be written as

$$\langle \delta_{RR_{st}(\tau)} \delta_{R'R_{st}(\tau')} \rangle = P(R, \tau; R', \tau'), \quad (43a)$$

$$= P(R, \tau | R', \tau') P_{R'}(\tau'), \quad (43b)$$

$$= P(R, \tau | R', \tau') P_{R'}^\infty. \quad (43c)$$

By definition,  $P(R, \tau; R', \tau')$  is the joint probability for observing successively the bath in the states  $R'$  and  $R$  at times  $\tau'$  and  $\tau$  respectively ( $\tau > \tau'$ ). By using the Markov property of the underlying bath fluctuations it can be expressed in terms of the conditional probability  $P(R, \tau | R', \tau')$  [7]. As before, for simplifying the analysis, in the third line of the previous equation we assumed that the bath fluctuations begin in their stationary state.

The second line of Eq. (42) define the correlation of the counting processes  $\{n_R^{st}(\tau)\}$ . Due to the statistical independence of these objects, when  $R \neq R'$  it follows  $\overline{n_R^{st}(\tau) n_{R'}^{st}(\tau')} = \overline{n_R^{st}(\tau)} \overline{n_{R'}^{st}(\tau')} = I_R I_{R'} \tau \tau'$ . After some manipulation, the second cumulant (41) reads

$$\begin{aligned} \langle\langle \Delta n_{st}^2(t) \rangle\rangle_{\{P\}} &= 2 \sum_R \int_0^t d\tau \int_0^\tau d\tau' \frac{d}{d\tau} \frac{d}{d\tau'} \overline{\Delta n_R^2(\tau, \tau')} \quad (44) \\ &\quad \times P(R, \tau | R, \tau') P_R^\infty + 2 \sum_{RR'} I_R I_{R'} f_{RR'}(t), \end{aligned}$$

where we have introduced the matrix of functions

$$f_{RR'}(t) = \int_0^t d\tau \int_0^\tau d\tau' [P(R, \tau | R', \tau') - P_R^\infty] P_{R'}^\infty, \quad (45)$$

and the diagonal correlation  $\overline{\Delta n_R^2(\tau, \tau')} = \overline{n_R^{st}(\tau) n_R^{st}(\tau')} - \overline{n_R^{st}(\tau)} \overline{n_R^{st}(\tau')}$ . The correlation time of this object is much smaller than the bath transition time. Hence, we can approximate  $(d/d\tau') \overline{\Delta n_R^2(\tau, \tau')} \approx \delta(\tau - \tau') \overline{\Delta n_R^2(\tau, \tau)} = \delta(\tau - \tau') \overline{\Delta n_R^2(\tau)}$ , where

$$\overline{\Delta n_R^2(\tau)} = \overline{n_R^{st}(\tau) n_R^{st}(\tau)} - \overline{n_R^{st}(\tau)} \overline{n_R^{st}(\tau)}, \quad (46)$$

is the second cumulant of each process  $n_R^{st}(\tau)$ . From Eq. (44) we get the final expression

$$\langle\langle \Delta n_{st}^2(t) \rangle\rangle_{\{P\}} = \sum_R P_R^\infty \overline{\Delta n_R^2}(t) + 2 \sum_{RR'} I_R I_{R'} f_{RR'}(t). \quad (47)$$

We notice that in addition to the linear combination given by the first contribution,  $\langle\langle \Delta n_{st}^2(t) \rangle\rangle_{\{P\}}$  is also proportional to the intensities  $\{I_R\}$ . The normalized cumulant  $\langle\langle \Delta n_{st}^2 \rangle\rangle = \lim_{t \rightarrow \infty} (1/t) \langle\langle \Delta n_{st}^2(t) \rangle\rangle$  reads

$$\langle\langle \Delta n_{st}^2 \rangle\rangle_{\{P\}} = \sum_R P_R^\infty \overline{\Delta n_R^2} + 2 \sum_{RR'} I_R I_{R'} f_{RR'}. \quad (48)$$

The matrix  $f_{RR'}$  is given by

$$f_{RR'} \equiv \lim_{t \rightarrow \infty} \frac{1}{t} f_{RR'}(t), \quad (49)$$

the intensities  $\{I_R\}$  follows from Eq. (29) and

$$\overline{\Delta n_R^2} = I_R \left[ 1 - \frac{(6\gamma_R^2 - 8\delta_R^2)\Omega_R^2}{(\gamma_R^2 + 2\Omega_R^2 + 4\delta_R^2)^2} \right], \quad (50)$$

where as before  $\delta_R = \omega_L - \omega_R$ . This expression, as well as that for the set  $\{I_R\}$ , satisfy the relations

$$I_R = \left. \frac{\partial \Theta'_M(s)}{\partial s} \right|_{s=0}, \quad \overline{\Delta n_R^2} = - \left. \frac{\partial^2 \Theta'_M(s)}{\partial s^2} \right|_{s=0}, \quad (51)$$

where  $\Theta'_M$  is the grand potential associated to Eq. (33) under the replacements  $\omega \rightarrow \omega_R$ ,  $\Omega \rightarrow \Omega_R$ , and  $\gamma \rightarrow \gamma_R$ .

For a two-dimensional configurational bath space,  $R = A, B$ , the constants (49) can easily be written as  $f_{RR'} = (2\delta_{RR'} - 1) P_A^\infty P_B^\infty$ . From Eq. (48), we get

$$\langle\langle \Delta n_{st}^2 \rangle\rangle_{\{P\}} = \sum_{R=A,B} P_R^\infty \overline{\Delta n_R^2} + 2 \frac{P_A^\infty P_B^\infty (I_A - I_B)^2}{(\phi_{AB} + \phi_{BA})}, \quad (52)$$

where  $P_A^\infty = \phi_{AB}/(\phi_{AB} + \phi_{BA})$  and  $P_B^\infty = \phi_{BA}/(\phi_{AB} + \phi_{BA})$ . We notice that these expressions recover the results obtained in Ref. [16] through a different approach.

## B. Extension to the thermodynamic approach

The previous stochastic approach describes the  $s$ -ensemble in  $s = 0$ , i.e., in a slow modulation limit it can fit the statistical behavior dictated by the probabilities  $\{P_n(t)\}$  [Eq. (21)] or equivalently the states  $\{\rho_R(t)\}$  [Eq. (15)]. For  $s \neq 0$ , it does not apply. In this case, the relevant objects are the probabilities  $\{q_n(t)\}$  [Eq. (2)] and the states  $\{\tilde{\rho}_R(t)\}$  [Eq. (27)]. In the following calculations, we assume that the slow modulation limit and the stochastic approach can also be applied for any value of the pseudo chemical potential  $s$ . The consistency of this ansatz relies on the results that can be obtained from it.

By noting that  $\langle\langle n_{st} \rangle\rangle_{\{P\}} = \langle\langle N \rangle\rangle|_{s=0}$ , from Eq. (40), we write the first  $s$ -dependent cumulant as

$$\langle\langle N \rangle\rangle \simeq \sum_R \tilde{P}_R^\infty(s) \langle\langle N_R \rangle\rangle, \quad (53)$$

where consistently  $\langle\langle N_R \rangle\rangle \equiv \langle\langle N \rangle\rangle'_M$ . Here,  $\langle\langle N \rangle\rangle'_M$  is defined by Eq. (34) after replacing  $\omega \rightarrow \omega_R$ ,  $\Omega \rightarrow \Omega_R$ , and  $\gamma \rightarrow \gamma_R$ . On the other hand, here the weights are

$$\tilde{P}_R^\infty(s) \equiv \lim_{t \rightarrow \infty} \text{Tr}[\tilde{\rho}_R(t)], \quad (54)$$

where  $\tilde{\rho}_R(t)$  is defined by (27).

Taking into account that  $\langle\langle\Delta n_{st}^2\rangle\rangle_{\{P\}} = \langle\langle\Delta N^2\rangle\rangle|_{s=0}$ , from Eq. (47) we propose the expression

$$\langle\langle\Delta N^2\rangle\rangle \simeq \sum_R \tilde{P}_R^\infty(s) \langle\langle\Delta N_R^2\rangle\rangle + 2 \sum_{RR'} \langle\langle N_R \rangle\rangle \langle\langle N_{R'} \rangle\rangle \tilde{f}_{RR'}(s), \quad (55)$$

where  $\langle\langle\Delta N_R^2\rangle\rangle \equiv \langle\langle\Delta N^2\rangle\rangle'_M$  also follows from Eq. (34) after replacing  $\omega \rightarrow \omega_R$ ,  $\Omega \rightarrow \Omega_R$ , and  $\gamma \rightarrow \gamma_R$ .

The expressions (53) and (55) depend on the stationary populations (54) and the generalized matrix  $\tilde{f}_{RR'}(s)$ . Its definition can read from Eq. (49) after introducing in Eq. (45) the  $s$ -dependence of the bath populations [ $P_R \rightarrow \tilde{P}_R(s)$ ]. The exact expressions for these objects for arbitrary bath spaces [Eq. (14)] are very complicated and do not provide an intuitive frame for understanding the thermodynamics of the  $s$ -ensemble. Therefore, from now on we restrict to a two-dimensional reservoir,  $R = A, B$ . From Eq. (52) we write

$$\langle\langle\Delta N^2\rangle\rangle \simeq \sum_{R=A,B} \tilde{P}_R^\infty(s) \langle\langle\Delta N_R^2\rangle\rangle + 2 \frac{\tilde{P}_A^\infty(s) \tilde{P}_B^\infty(s)}{\tilde{\phi}(s)} \times (\langle\langle N_A \rangle\rangle - \langle\langle N_B \rangle\rangle)^2, \quad (56)$$

where  $\tilde{\phi}(s) = \tilde{\phi}_{AB}(s) + \tilde{\phi}_{BA}(s)$ .

Eqs. (53) and (56) only depends on the stationary populations  $\{\tilde{P}_R^\infty(s)\}$  and the generalized rate  $\tilde{\phi}(s)$ . These functions can be approximated in the following way. Consistently with an equilibrium thermodynamic approach, the populations are expressed as

$$\tilde{P}_A^\infty(s) \simeq \frac{e^{-(\zeta_A + \xi_A(s))}}{\mathcal{Z}(s)}, \quad \tilde{P}_B^\infty(s) \simeq \frac{e^{-(\zeta_B + \xi_B(s))}}{\mathcal{Z}(s)}, \quad (57)$$

where  $\zeta_R + \xi_R(s)$  is the ‘‘energy’’ associated to each  $R$ -bath state. This splitting is defined such that  $\xi_R(0) = 0$ . On the other hand, the function  $\mathcal{Z}(s)$  guarantees the normalization  $\tilde{P}_A^\infty(s) + \tilde{P}_B^\infty(s) = 1$ . Then, we can rewrite

$$\tilde{P}_A^\infty(s) \simeq \frac{1}{2} \{1 - \tanh[\varepsilon_0 + \varepsilon(s)]\}, \quad (58a)$$

$$\tilde{P}_B^\infty(s) \simeq \frac{1}{2} \{1 + \tanh[\varepsilon_0 + \varepsilon(s)]\}, \quad (58b)$$

where  $\varepsilon_0 = (\zeta_A - \zeta_B)/2$ , and  $\varepsilon(s) = [\xi_A(s) - \xi_B(s)]/2$ . In  $s = 0$ , these expressions must to satisfy the condition  $\tilde{P}_R^\infty(0) = P_R^\infty$ , which imply the expression

$$\varepsilon_0 = \frac{1}{2} \log \left[ \frac{P_B^\infty}{P_A^\infty} \right] = \frac{1}{2} \log \left[ \frac{\phi_{BA}}{\phi_{AB}} \right]. \quad (59)$$

On the other hand, the dependence of  $\varepsilon(s)$  is assumed to be linear in  $s$ , i.e.,  $\varepsilon(s) \simeq s\delta\varepsilon$ . The constant  $\delta\varepsilon$  can be determine from the relation between Eqs. (53) and (55)

in  $s = 0$ , i.e.,  $(\partial/\partial s)\langle\langle N \rangle\rangle|_{s=0} = -\langle\langle\Delta N^2\rangle\rangle|_{s=0}$ . After some algebra, from Eq. (56), it follows

$$\varepsilon(s) \simeq s \delta\varepsilon = s \frac{I_A - I_B}{\phi_{AB} + \phi_{BA}}. \quad (60)$$

Both  $\varepsilon_0$  and  $\delta\varepsilon$  may assume positive and negative values.

The generalized rate  $\tilde{\phi}(s)$  [Eq. (56)] defines the characteristic decay time of the  $s$ -dependent bath populations. It must to satisfies the conditions  $\tilde{\phi}(s) \geq 0$  and  $\tilde{\phi}(0) = (\phi_{AB} + \phi_{BA})$ . We assume the dependence

$$\tilde{\phi}(s) \simeq \alpha s(s - 2s_p) + (\phi_{AB} + \phi_{BA}), \quad (61)$$

where  $s_p$  is a dimensionless parameter while  $\alpha \geq 0$ , as well as  $\tilde{\phi}(s)$ , has units of [1/time]. As a function of  $s$ , the rate  $\tilde{\phi}(s)$  reaches its minimal value at  $s = s_p$ . This constant is chosen as the value of  $s$  at which the second contribution of Eq. (56) reaches its maximal value. It can be approximated by the value at which the function  $\tilde{P}_A^\infty(s) \tilde{P}_B^\infty(s) = 1/(2 \cosh[\varepsilon_0 + \varepsilon(s)])^2$  is maximal. Hence, we take

$$s_p = -\frac{\varepsilon_0}{\delta\varepsilon} = \frac{(\phi_{AB} + \phi_{BA})}{2(I_A - I_B)} \log \left[ \frac{P_A^\infty}{P_B^\infty} \right]. \quad (62)$$

Finally, the coefficient  $\alpha$  can be determine from the condition  $(\partial/\partial s)\langle\langle\Delta N^2\rangle\rangle|_{s=0} = -\langle\langle\Delta N^2\rangle\rangle|_{s=0}$ . Alternatively, due to its large size expression, it can be considered as a free fitting parameter.

The  $s$ -extension of the stochastic approach allows us to get closed expressions [Eqs. (53) and (56)] for approximating the thermodynamic approach in the slow modulation limit. In Fig. 2 we plot the average number and the normalized fluctuations obtained from Eqs. (13), (23) and (25). As in the previous section, the configurational bath space is two-dimensional,  $R = A, B$ . It only affects the natural decay of the system,  $\{\gamma_R\}$ . Hence, we take  $\omega_R = \omega_0$ ,  $\Omega_R = \Omega$ , and  $\omega_L = \omega_0$ , i.e., the spectral shifts are null, the system-laser interaction is independent of the bath states, and the laser excitation is in resonance with the system.

In Fig. 2(a) we plot  $\langle\langle N \rangle\rangle$  as a function of  $s$ . The full (black) curve is the (exact) numerical solution obtained from Eqs. (13), (23), and (25). The grand potential  $\Theta(s)$  follows from the larger root of an eighth order polynomial function. The dotted (black) curves (indistinguishable) correspond to the fitting arising from the stochastic approach, Eq. (53). In the scale of the plot, we note that the average number can be approximated as

$$\langle\langle N \rangle\rangle \approx \begin{cases} \langle\langle N_A \rangle\rangle & \text{for } s < 0 \\ \langle\langle N_B \rangle\rangle & \text{for } s > 0 \end{cases}, \quad (I_A > I_B). \quad (63)$$

The superposed blue squares and red circles curves correspond to  $\langle\langle N_A \rangle\rangle$  and  $\langle\langle N_B \rangle\rangle$  respectively. These contributions follow as the first derivative with respect to  $s$  of the grand potential  $\Theta_M(s)$ , Eq. (35), under the replacement  $\gamma \rightarrow \gamma_R$ . The (crude) approximation (63) implies



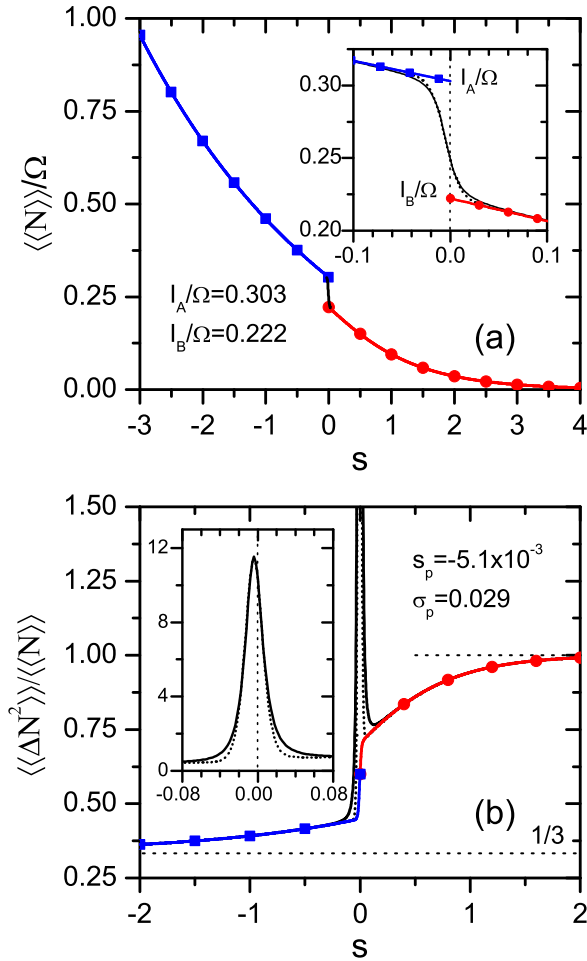


FIG. 2: (color online) Average number value  $\langle\langle N \rangle\rangle$  and normalized fluctuations  $\langle\langle \Delta N^2 \rangle\rangle/\langle\langle N \rangle\rangle$  as a function of  $s$  in the slow modulation limit. The insets show the behaviors around  $s \approx 0$ . The full (black) curves correspond to the numerical solutions associated to Eqs. (13), (23), and (25). The dotted (black) curves are the fitting obtained from the stochastic approach, Eqs. (53) and (56). In (a) the blue squares and red circles correspond respectively to  $\langle\langle N_A \rangle\rangle$  and  $\langle\langle N_B \rangle\rangle$  determined from Eqs. (34) and (35). In (b) the blue squares and red circles correspond to  $\langle\langle \Delta N_A^2 \rangle\rangle/\langle\langle N \rangle\rangle$  and  $\langle\langle \Delta N_B^2 \rangle\rangle/\langle\langle N \rangle\rangle$ . The parameters are  $\omega_R = \omega_0$ ,  $\Omega_R = \Omega$ ,  $\omega_L = \omega_0$ ,  $\gamma_A/\Omega = 2.5$ ,  $\gamma_B/\Omega = 0.5$ ,  $\phi_{AB}/\Omega = 4 \times 10^{-4}$ ,  $\phi_{BA}/\Omega = 8 \times 10^{-4}$ , and  $\alpha/\Omega = 2.15$ .

that [see Eq. (53)]  $\tilde{P}_A^\infty(s) \approx \theta(-s)$  and  $\tilde{P}_B^\infty(s) \approx \theta(s)$ , where  $\theta(s)$  is the step function [ $\theta(s) = 0$  for  $s < 0$  and  $\theta(s) = 1$  for  $s > 0$ ]. As the values of the decay rates [ $\gamma_A/\Omega = 2.5$ ,  $\gamma_B/\Omega = 0.5$ ] correspond to the average values of Fig. 1, the behavior of  $\langle\langle N_A \rangle\rangle$  and  $\langle\langle N_B \rangle\rangle$  for any value of  $s$  can also be read from that plot.

Consistently with the approximation (63), the behavior of  $\langle\langle N \rangle\rangle$  around  $s \approx 0$  seems to be discontinuous. We notice that a similar behavior arises in thermodynamical first-order transitions. For example, if a transition is driven by temperature, the discontinuity in the derivative of the thermodynamic potential may

corresponds to the difference of specific volume of two coexisting phases [21]. Here, the “jump” in  $\langle\langle N \rangle\rangle$  is  $(\langle\langle N_A \rangle\rangle - \langle\langle N_B \rangle\rangle)|_{s=0} = I_A - I_B$ . Hence, two thermodynamic phases can be associated to the intensity regimes defined by  $\langle\langle N_A \rangle\rangle$  and  $\langle\langle N_B \rangle\rangle$ .

While the average  $\langle\langle N \rangle\rangle$  seems to be a discontinuous function on a large  $s$ -scale, around the origin it is a continuous function of  $s$ . This property is shown in the inset of Fig. 2(a). Even at those small scales, the stochastic approach, Eq. (53), provides an indistinguishable fitting (black dotted curve). In thermodynamical systems, finite-size effects produce a similar smoothing of the free energy derivative [29–32]. In the present case, this relation is established in the following section.

In Fig. 2(b) we plot the normalized fluctuations  $\langle\langle \Delta N^2 \rangle\rangle/\langle\langle N \rangle\rangle$  as a function of  $s$ . Consistently with the rough approximation (63), on larger  $s$ -scales we expect the validity of the approximation

$$\langle\langle \Delta N^2 \rangle\rangle \approx \begin{cases} \langle\langle \Delta N_A^2 \rangle\rangle & \text{for } s < 0 \\ \langle\langle \Delta N_B^2 \rangle\rangle & \text{for } s > 0 \end{cases}, \quad (I_A > I_B), \quad (64)$$

where  $\langle\langle \Delta N_R^2 \rangle\rangle$  follows from Eqs. (34) and (35). The superposed blue squares and red circles curves correspond to this approximation. While they provide a very good fitting for  $|s| > 0$ , around the origin the fluctuations develops a narrow and abrupt peak (see the inset). The stochastic approach (black dotted line) also fits this property.

The background behavior and the peak in  $\langle\langle \Delta N^2 \rangle\rangle$  can be read from Eq. (56). In fact, the crude approximation (64) is indistinguishable from the contribution  $\sum_{R=A,B} \tilde{P}_R^\infty(s) \langle\langle \Delta N_R^2 \rangle\rangle$ . On the other hand, the narrow peak is fitted by the contribution proportional to the product of the stationary populations  $\tilde{P}_A^\infty(s) \tilde{P}_B^\infty(s) = 1/(2 \cosh[\varepsilon_0 + \varepsilon(s)])^2$ . Therefore, the maximal value of the peak occurs at  $s = s_p$ , Eq. (62), i.e., the value of  $s$  at which  $\tilde{P}_A^\infty(s) = \tilde{P}_B^\infty(s) = 1/2$ . The inset of Fig. 2(b) confirms this prediction. Furthermore, from Eq. (56) the value of  $\langle\langle \Delta N^2 \rangle\rangle$  at  $s_p$  can be approximated as

$$\langle\langle \Delta N^2 \rangle\rangle|_{s=s_p} \approx \frac{1}{2} \sum_{R=A,B} \overline{\Delta n_R^2} + \frac{(I_A - I_B)^2}{2(\phi_{AB} + \phi_{BA})}, \quad (65)$$

$[\langle\langle N \rangle\rangle|_{s=s_p} \approx (I_A + I_B)/2]$ , while the width of the peak,  $\sigma_p$ , can be estimated as

$$\sigma_p \approx 2 \frac{(\phi_{AB} + \phi_{BA})}{|I_A - I_B|}. \quad (66)$$

Taking different values of the parameters of the evolution (25), we have checked that in the slow modulation limit the position, height and width of the peak obey the scaling defined by Eqs. (62), (65), and (66) respectively. From these expressions, one can deduce that in the limit  $(\phi_{AB} + \phi_{BA}) \rightarrow 0$ , the peak becomes proportional to a delta Dirac function. Therefore, asymptotically a first-order transition happens. The thermodynamic response

functions, for all values of  $s$ , are given by Eqs. (63) and (64), i.e., the grand potential is  $\Theta(s) = \Theta_A(s)$  for  $s < 0$ ,  $\Theta(s) = \Theta_B(s)$  for  $s > 0$ , with  $\Theta(0) = 0$ .

### C. Finite-size effects and double-Gaussian approximation

Finite-size effects in first-order transitions [29, 30] has been analyzed for systems such as the Ising [31] and  $q$ -state Potts models [32]. While in these systems the transition is driven by a magnetic field or temperature, the thermodynamic functions have similar behaviors to those shown in Fig 2. The scaling of the peak in the second derivative of the thermodynamic potential [32] is similar to those of Eqs. (62), (65), and (66).

From a theoretical point of view, finite-size effects at first-order transitions can be characterized over the basis of (equilibrium) Einstein fluctuation theory [21], which provides the probability distribution of the thermodynamic variable fluctuations. For example, for an open (thermal) system, the probability distribution  $\mathcal{P}(N)$  of the particle number is a Gaussian distribution  $\mathcal{P}(N) = [2\pi kT(\partial/\partial\mu)\bar{N}]^{-1/2} \exp[-(N - \bar{N})^2/2kT(\partial/\partial\mu)\bar{N}]$ , where  $T$  is the temperature,  $\bar{N}$  is the average particle number and  $\mu$  is the chemical potential.

In the present approach, the transition is driven by the pseudo chemical potential  $s$  and the size of the system must to be inversely proportional to the rate of the bath fluctuations. Consistently with the Einstein fluctuation theory, we search for a probability distribution  $\mathcal{P}(N)$ , with  $\int_{-\infty}^{+\infty} \mathcal{P}(N)dN = 1$ , such that the average number can be obtained as

$$\langle\langle N \rangle\rangle = \int_{-\infty}^{+\infty} \mathcal{P}(N)NdN, \quad (67)$$

while the second cumulant follows from

$$\langle\langle \Delta N^2 \rangle\rangle = \frac{1}{\Upsilon(s)} \int_{-\infty}^{+\infty} \mathcal{P}(N)(N - \langle\langle N \rangle\rangle)^2 dN. \quad (68)$$

Here, the inverse of  $\Upsilon(s)$  measures the ‘‘size’’ of the system [32]. In an infinite-size limit,  $\mathcal{P}(N)$  must be a Gaussian distribution [21]. Nevertheless, when finite-size effects are considered in a first-order transition, one must to consider a superposition of Gaussian distributions, each one representing the coexisting phases [32]. In fact, the different phases are randomly explored by the system when its size is finite [32]. This effect is similar to the blinking property of the slow modulation limit [19, 20].

In our problem, the coexistent phases correspond to the different intensity regimes defined by  $\langle\langle N_R \rangle\rangle$ . Then,

$$\mathcal{P}(N) = \frac{\tilde{P}_A^\infty(s)}{\sqrt{2\pi\langle\langle \Delta N_A^2 \rangle\rangle\Upsilon(s)}} \exp\left[-\frac{(N - \langle\langle N_A \rangle\rangle)^2}{2\langle\langle \Delta N_A^2 \rangle\rangle\Upsilon(s)}\right] + \frac{\tilde{P}_B^\infty(s)}{\sqrt{2\pi\langle\langle \Delta N_B^2 \rangle\rangle\Upsilon(s)}} \exp\left[-\frac{(N - \langle\langle N_B \rangle\rangle)^2}{2\langle\langle \Delta N_B^2 \rangle\rangle\Upsilon(s)}\right]. \quad (69)$$

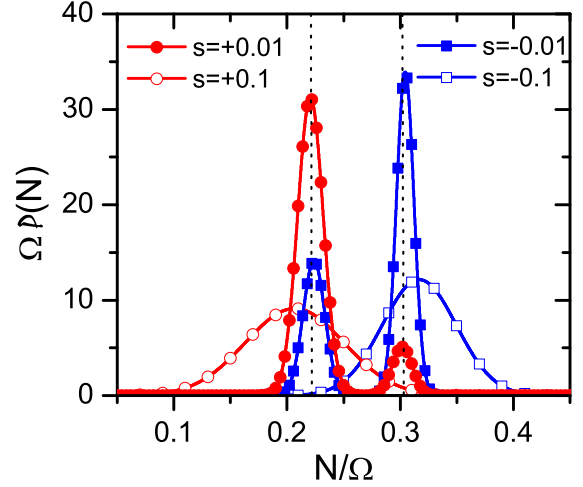


FIG. 3: (color online) Probability distribution (69) for different values of  $s$ . The vertical dotted lines correspond to  $N/\Omega = I_A/\Omega = 0.303$ , and  $N/\Omega = I_B/\Omega = 0.222$ . The parameters are the same than in Fig. 2.

Here,  $\langle\langle N_R \rangle\rangle$  and  $\langle\langle \Delta N_R^2 \rangle\rangle$  follows from Eq. (34) while  $\Upsilon(s) = \tilde{\phi}(s)/2$  [Eq. (61)]. Furthermore, the weight of each Gaussian distribution is expressed in terms of the thermodynamic potential of each phase [32]. Therefore, the populations  $\tilde{P}_R^\infty(s)$  are written as  $\tilde{P}_R^\infty(s) \simeq \exp[-\zeta_R - \Theta_R(s)/\tilde{\phi}(s)]/\mathcal{Z}(s)$ , where  $\mathcal{Z}(s)$  guarantees the normalization  $\tilde{P}_A^\infty(s) + \tilde{P}_B^\infty(s) = 1$  [compare with (57)] and  $\Theta_R(s)$  is the grand potential of each phase. For the example shown in Fig. 2, these functions can be read from Eq. (35) under the replacement  $\gamma \rightarrow \gamma_R$ . Trivially, the populations  $\tilde{P}_R^\infty(s)$  can be rewritten as in Eq. (58) with  $\varepsilon_0$  defined by Eq. (59) and

$$\varepsilon(s) \approx \frac{\Theta_A(s) - \Theta_B(s)}{\tilde{\phi}(s)} \approx s \frac{I_A - I_B}{(\phi_{AB} + \phi_{BA})} + O(s^2). \quad (70)$$

This result recovers Eq. (60) and proofs the consistency of the previous results and scaling. In fact, the double-Gaussian probability distribution (69), through Eqs. (67) and (68), recovers the expressions of the extended stochastic approach, Eqs. (53) and (56) respectively.

In Fig. 3 we plot the distribution (69) for different values of  $s$ . The parameters of the underlying evolution are the same than in Fig. 2. Near of the transition,  $s \approx s_p \approx 0$ , the probability distribution is a double-Gaussian one. Consistently, the higher peaks are centered around the values  $N \approx I_A$  ( $s < 0$ ) and  $N \approx I_B$  ( $s > 0$ ). For  $|s| \gg s_p$ , the distribution has only one peak, which is centered around  $s \approx \langle\langle N_R \rangle\rangle$ .

The double-Gaussian approximation, and consistently the stochastic approach, can be extended beyond the slow modulation limit. Nevertheless, parameters such as the position  $s_p$  and width  $\sigma_p$  of the peak must be taken as free parameters. For example, a reasonable fitting is obtained after replacing the polynomial function (61) with

an hyperbolic one and introducing a non-linear function  $\varepsilon(s)$ , both of them defined with extra free parameters.

## VI. SUMMARY AND CONCLUSIONS

The (non-equilibrium) ensemble of measurement realizations of an open quantum system can be analyzed with the LD formalism. For fluorescent systems under a direct photon detection scheme, this approach allow to describe the asymptotic behavior of the photon counting probabilities through a thermodynamic-like formalism [22]. In this paper we have studied the thermodynamic approach associated to a fluorescent system coupled to a complex self-fluctuating environment able to modify the characteristic parameters of the system evolution.

The statistical mechanics underlying the thermodynamic frame is defined by a set of auxiliary probabilities whose characteristic events are the unlikely ones of the photon counting realizations, Eq. (2). A free energy function, Eq. (9), through a Legendre transformation, defines the long time behavior of the photon counting probabilities. Here, its functional form follows from the trace of a generating function operator, Eq. (23), whose evolution, Eq. (25), takes into account the parameter fluctuations induced by the environment.

In a fast modulation limit, i.e., when the characteristic time of the environment fluctuations is much smaller than the time between consecutive photon emissions, the thermodynamic frame can be well approximated with that corresponding to a Markovian fluorescent system. Its evolution is defined by a set of parameters that follows from an average weighted by the stationary populations of each bath state, Eq. (30). When the bath only affects the natural decay of the system and the external laser excitation is in resonance with the system, the thermodynamic potential can be approximated by a simple analytical expression, Eq. (35). In this limit, the response functions do not display any property related to a phase transition. Nevertheless, the normalized fluctuations always interpolate between a scale invariant regime and a Poissonian one [Fig. 1].

In the slow modulation limit, the fluorescent signal is characterized by a blinking phenomenon. The scattered intensity randomly changes between a set of values associated to each bath state, Eq. (29). The photon counting process can be approximated by the product of two kind of statistically independent stochastic variables, one related to the quantum photon emission process and the other to the bath fluctuations, Eq. (37). In the ther-

modynamic frame, each intensity regime can be read as a different thermodynamic phase. A natural extension of the stochastic approach provides the basis for characterizing its statistical properties. After imposing some consistency relations, the average number is written as a linear combination of the values corresponding to each phase, Eq. (53). The fluctuations around the average number can be approximated in a similar way, Eq. (56).

The behavior of the average number and the centered fluctuations is similar to that found in finite-size systems near a first-order phase transition. This is the main result of this contribution. Instead of a discontinuity in the first derivative of the thermodynamic potential, an abrupt but continuous change in its slope is observed. Furthermore, the second derivative, instead of a delta Dirac contribution, displays a narrow peak [Fig. 2]. These effects are controlled by the size of the system, which is proportional to the transition rate between the bath states. The location, height and width of the peak obey the scaling properties obtained from the stochastic approach, i.e., Eqs. (62), (65), and (66) respectively. The finite-size effects can also be obtained from a generalization of the Einstein's fluctuations theory. The probability distribution of the fluctuations follows from a double-Gaussian distribution [Eq. (69)], each contribution being related to each coexisting phase [Fig. 3].

From our results, we conclude that whenever a (photon) counting process has an underlying blinking property, the thermodynamic approach is characterized by finite-size effects corresponding to a first-order transition. Therefore, the studied phenomena, for example, must also appear when the blinking properties depend on the external laser excitation, i.e., for light assisted processes [19, 20]. These and previous results [22] confirm that diverse thermodynamical properties of many body (equilibrium) systems are also present in the statistical properties of (non-equilibrium) quantum measurement trajectories. This mapping raise up fundamental physical questions such as the possibility of simulating complex dynamics with simple open quantum systems subjected to a continuous measurement process.

## Acknowledgments

The author thanks fruitful discussions with M. Fiori, E. Urdapilleta, and L. Quiroga Puello. This work was supported by CONICET, Argentina, PIP 11420090100211.

- 
- [1] H.P. Breuer and F. Petruccione, *The Theory of Open Quantum Systems*, (Oxford University Press, 2002).  
 [2] M.B. Plenio and P.L. Knight, *Rev. Mod. Phys.* **70**, 101 (1998).

- [3] H.J. Carmichael, *An Open Systems Approach to Quantum Optics*, Lecture Notes in Physics, Vol. M18, (Springer, Berlin, 1993).  
 [4] A. Barchielli and M. Gregoratti, *Quantum Trajectories*

- and Measurements in Continuous time—The diffusive case, Lectures Notes in Physics, Vol. **782** (Springer, Berlin, 2009).
- [5] D.F. Walls and G.J. Milburn, *Quantum Optics* (Springer-Verlag, Berlin, 1994).
- [6] L. Mandel and E. Wolf, *Optical coherence and quantum optics* (Cambridge University press, 1995).
- [7] N.G. van Kampen, *Stochastic Processes in Physics and Chemistry*, (Sec. Ed., North-Holland, Amsterdam, 1992).
- [8] R.J. Cook, Phys. Rev. A **23**, 1243 (1981); S. Mukamel, Phys. Rev. A **68**, 063821 (2003).
- [9] E. Barkai, Y. Jung, and R. Silbey, Annu. Rev. Phys. Chem. **55**, 457 (2004).
- [10] M. Lippitz, F. Kulzer, and M. Orrit, Chem. Phys. Chem. **6**, 770 (2005).
- [11] Y. Jung, E. Barkai, and R.J. Silbey, J. Chem. Phys. **117**, 10980 (2002).
- [12] Y. Zheng and F.L. Brown, Phys. Rev. Lett. **90**, 238305 (2003).
- [13] Y. He and E. Barkai, Phys. Rev. Lett. **93**, 068302 (2004).
- [14] Y. He and E. Barkai, J. Chem. Phys. **122**, 184703 (2005).
- [15] F.L. Brown, Phys. Rev. Lett. **90**, 028302 (2003).
- [16] Y. Zheng and F.L.H. Brown, J. Chem. Phys. **121**, 7914 (2004).
- [17] A.A. Budini, Phys. Rev. A **73**, 061802(R) (2006); J. Chem. Phys. **126**, 054101 (2007); J. Phys. B **40**, 2671 (2007); Phys. Rev. A **76**, 023825 (2007).
- [18] I.S. Osad'ko and V.V. Fedyanin, J. Chem. Phys. **130**, 064904 (2009); I.S. Osad'ko, J. Chem. Phys. **131**, 185101 (2009).
- [19] A.A. Budini, Phys. Rev. A **79**, 043804 (2009).
- [20] A.A. Budini, J. Phys. B: At. Mol. Phys. **43**, 115501 (2010).
- [21] L.E. Reichl, *A Modern Course in Statistical Physics* (J. Wiley and Sons, New York 2nd ed., 1998).
- [22] J.P. Garrahan and I. Lesanovsky, Phys. Rev. Lett. **104**, 160601 (2010).
- [23] H. Touchette, Phys. Rep. **478**, 1 (2009).
- [24] J.P. Garrahan., R.L. Jack, V. Lecomte, E. Pitard, K. van Duijvendijk, and F. van Wijland, J. Phys. A **42**, 075007 (2009).
- [25] J. Hooyberghs and C. Vanderzande, J. Stat. Mech. P02017 (2010).
- [26] R. Jack and P. Sollich, Prog. Theor. Phys. Supp. **184**, 304 (2010).
- [27] R.M.L. Evans, Phys. Rev. Lett. **92**, 150601 (2004).
- [28] J.P. Garrahan, R.L. Jack, V. Lecomte, E. Pitard, K. van Duijvendijk, and F. van Wijland, Phys. Rev. Lett. **98**, 195702 (2007).
- [29] K. Binder and D.W. Heermann, *Monte Carlo Simulation in Statistical Physics: An introduction*, Springer Series in Solid-State Sciences 80 (Springer-Verlag, Berlin, 1988).
- [30] K. Binder, Rep. Prog. Phys. **50**, 783 (1987).
- [31] K. Binder and D.P. Landau, Phys. Rev. B **30**, 1477 (1984).
- [32] M.S.S. Challa, D.P. Landau, and K. Binder, Phys. Rev. B **34**, 1841 (1986).